CMLS, Cell. Mol. Life Sci. 61 (2004) 1935–1945
1420-682X/04/151935-11
DOI 10.1007/s00018-004-4137-5

CMLS Cellular and Molecular Life Sciences

Research Article

Differential chemotactic potential of mouse platelet basic protein for thymocyte subsets

W. X. Fu, S. Y. Gong, X. P. Qian, Y. Li, M. L. Zhu, X. Y. Dong, Y. Li and W. F. Chen *

Department of Immunology, Peking University Health Science Center, Beijing 100083 (China),
Fax: +86 10 8280 1436; e-mail: wfchen@public.bta.net.cn

Received 25 March 2004; received after revision 10 May 2004; accepted 8 June 2004

Abstract. Mouse platelet basic protein (CXCL7/mPBP) was cloned from thymic stromal cells and further identification indicated that it was expressed in thymic monocytes/macrophages (Mo/Mϕs). Recombinant mPBP was chemoattractive for target cells of polymorphonuclear leucocytes, peritoneal Mo/Mϕs and splenic lymphocytes with distinct potencies. CXCR2 was identified to be a cognate receptor for mPBP. Mouse thymocyte subsets of $CD4^-CD8^-$ double-negative (DN), $CD4^+CD8^+$ double-positive (DP), $CD4^+CD8^-$ single-positive (CD4SP) and $CD4^-CD8^+$ single-positive (CD8SP) expressed cell surface CXCR2 with different positive percentages and expression levels. mPBP was chemoattractive for thymocyte subsets with the potency order DN>DP>CD8SP>CD4SP, consistent with the levels of CXCR2 expressed on the respective cells. Thus, mPBP in thymus is functionally redundant with chemokine CXCL12/SDF-1. Moreover, our finding that thymic Mo/Mϕs can produce mPBP implies that they may have other functions apart from acting as scavengers in thymus.

Key words. Chemokine; chemotaxis; monocyte/macrophage; stromal cell; thymus.

Chemokines belong to a superfamily of many small cytokines with structural similarity and chemotactic activity. They are secreted by leukocytes and various types of stromal cells. According to the numbers and positions of conserved cysteine residues, chemokines are divided into CXC, CC, C and CX_3C subfamilies. Chemokines are chemoattractive for a broad spectrum of leukocytes and play a pivotal role in lymphocyte migration, recirculation, modulation of the immune response and leukocyte recruitment to inflammatory sites. Apart from chemotactic activity, chemokines promote hematopoiesis, regulate angiogenesis and block HIV infection [1–5].

In thymus, the migration of developing thymocytes is tightly regulated by chemokines in coordination with adhesive molecules and extracellular matrix proteins [6]. Developing thymocytes at different stages express discrete chemokine receptors and are attracted by different types of chemokines produced by local thymic stromal cells to migrate to the specialized thymic regions for differentiation. The common lymphocyte progenitors (CLPs) and $CD4^-CD8^-$ double-negative (DN) thymocytes are preferentially chemoattracted by CXCL12 (stromal derived-factor 1, SDF-1) [7, 8], the $CD4^+CD8^+$ double-positive (DP) thymocytes are attracted by CCL25 (thymus-expressed chemokine, TECK) [9] and CCL22 (macrophage-derived chemokine, MDC) [10, 11]. After positive selection, surviving $CD69^+$ DP thymocytes develop into $TCR\alpha\beta^+CD4^+CD8^-$ single-positive (CD4SP)/$CD4^-CD8^+$ single-positive (CD8SP) medullary-type thymocytes and migrate into thymic medulla, where they undergo a process of final-stage differentiation. During this process, the SP thymocytes at early stages are responsive to CCL22 [10] and CCL25 [9], whereas the SP thymocytes at late stages are responsive to CXCL10 [interferon (IFN)-inducible protein-10, IP-10] [12], CCL19 (EBI1-ligand chemokine, ELC) and

* Corresponding author.

CCL21 (secondary lymphoid tissue chemokine, SLC) [13, 14]. However, in chemokine- or chemokine receptor-deficient mice, such as CXCL12-, CXCR4-, CCR7- and CXCR2-deficient mice, intrathymic thymocyte development proceeds normally [15–18]. This suggests the presence of chemokines with functional redundancy in the thymus. The intrathymic trafficking of developing thymocytes is obligatory for the thymocytes at distinct stages migrating to and residing in the discrete microenvironments to accomplish the programmed differentiation [19]. Clearly, the functional redundancy of chemokines is required for the physiological differentiation of developing thymocytes. It is thus not surprising that an increasing number of chemokines are being discovered in thymus.

During our study of chemokines produced by mouse thymic stromal cells (MTSCs), we found that established MTSC lines and cultures of freshly isolated mouse thymic stromal cells (fMTSCs) produced multiple types of chemokines [12]. Beside the reported CXCL12 [20] and CXCL10 [21], we found that MTSCs also expressed CCL5 (regulated on activation normal T expressed and secreted, RANTES), CCL2 (monocyte chemotactic protein-1, MCP-1) and XCL1 (lymphotactin) [12]. We showed that IP-10 was produced substantially by cortical-type thymic epithelial cell lines and was chemotactic to DP thymocytes, whereas CCL2 was produced by a medullary-type thymic epithelial cell line 1 (MTEC1) and was chemotactic for CD4/CD8SP thymocytes [12]. In principle, there is a close match between the chemokine receptors expressed on developing thymocytes and the respective chemokines produced by thymic stromal cells in the discrete anatomical loci within thymus. The developing thymocytes at distinct stages are chemoattracted and reside in the differently specialized thymic niches.

In thymus, the roles of chemokines containing the glutamic acid-leucine-arginine (ELR) motif have not been studied extensively. In searches of the GenBank EST databases for ELR-containing chemokines, we identified a novel murine ELR^+ CXC chemokine produced by thymic stromal cells (GenBank accession No. AF219112). During our work, this chemokine was independently identified as a mouse homologue of human platelet basic protein (hPBP/CXCL7) [22] and neutrophil-activating peptide-2 (NAP-2) protein [23]. To avoid confusion, we refer to this chemokine as mouse PBP (mPBP). Previous studies have suggested that mPBP is specifically expressed in spleen [23]. The functions of and receptor(s) for mPBP are unknown. In this paper, we demonstrated that in the thymus, mPBP was produced by thymic monocytes/macrophages (Mo/Mϕs) and CXCR2 was a receptor for mPBP. Furthermore, our results suggest that mPBP has differential chemotactic potential on distinct thymocyte subsets, consistent with the expressed levels of CXCR2 on the respective thymocyte subsets. Our findings imply that the mPBP-CXCR2 chemokine-receptor pair is involved in functional connections between thymic Mo/Mϕ and various thymocytes.

Materials and methods

Mice and cell line

Four- to 6-week-old female BALB/c mice were obtained from the Animal Facility, Peking University Health Science Center. The HEK293 cell line was cultured in Dulbecco's modified Eagle's medium (DMEM) containing 10% fetal calf serum (FCS).

Chemokine and antibodies

Recombinant mouse CXCL2/3 (macrophage inflammatory protein 2, MIP-2, PEPRO TECH, Rocky Hill, N. J.); PerCP-conjugated rat anti-mouse CD8 and PE-conjugated rat anti-mouse CD4 (BD-PharMingen, Los Angeles, Calif.); goat anti-mouse CXCR2 pAb (a kind gift from Dr. R. M. Streiter); anti-Mac-1 mAb (produced by a hybridoma M1/70 and purified from the ascites); alkaline phosphatase (AP)-conjugated anti-DIG Ab (Roche Diagnostics, Basel, Switzerland); anti-mouse DEC-205 mAb (BD-PharMingen) and anti-ER-TR-4, -5, -7 mAbs (kind gifts from Dr. van Ewijk) were obtained from the indicated manufacturers or investigators. The rabbit antiserum against mPBP was raised by immunization of rabbits with recombinant mPBP. The secondary Abs were purchased from the indicated manufactures: horseradish peroxidase (HRP)-conjugated anti-rat IgG (ZhongShan Biotech, Beijing, China); AP- or HRP-conjugated anti-goat IgG and HRP-conjugated anti-rabbit IgG (Promega, Madison, Wisc.); conjugated and unconjugated isotype-matched control IgG (Southern Biotechnology, Birmingham, Ala.).

Isolation of various types of immune cells

The cultures of fMTSCs were prepared as described elsewhere [24]. Briefly, mouse thymuses were finely minced and cultured in DMEM containing 10% FCS. The cultures were replenished with fresh medium once a week. After 3 weeks culture, all the thymocytes and dendritic cells died off and the viable cells were a mixture of cultured thymic stromal cells. Neutrophils (polymorphonuclear leucocytes, PMNs) were collected from mouse heparinized peripheral blood and purified by Histopaque-1119 (Sigma, St. Louis, Mo.) density gradient centrifugation according to the user's manual. Splenic lymphocytes, including T and B cells were prepared from mouse spleens after removal of erythrocytes by lysing with NH_4Cl buffer and depletion of monocytes and macrophages by adhesion on the plastic surface of tissue culture plates. Peritoneal monocytes including a minor proportion of macrophages were collected from peritoneal cavities after injection into the cavity with 3 ml cooled

RPMI-1640 medium for 4 h. These cavity cells were further adhered on the plastic surface of tissue culture plates, the non-adhered cells were washed off and the adhered cells were scraped with a sterile cell scraper to obtain purified monocytes. The purity of isolated cell populations was more than 90% as analyzed by flow cytometry. To prepare Mo/Mϕs-depleted thymic stromal cells, we first prepared fresh thymic stromal cells from thymus cell suspension through the following steps: thymuses were cut to small fragments and digested with collagenase (1 mg/ml) and DNase I (30 IU /ml) to obtain a thymus cell suspension; the thymus cell suspension was adhered on the plastic surface of tissue culture plates, non-adherent thymocytes were washed off and the adherent thymic stromal cells were collected by scraping. MTSCs were stained with FITC-anti-Mac-1 mAb and sorted by flow cytometry (FACS Vantage, BD Biosciences, San Jose, Calif.) to collect both thymic Mo/Mϕs and thymic Mo/Mϕs-depleted stromal cells. DN, DP, CD4SP and CD8SP thymocytes were sorted from the thymocyte suspension after double-staining with PerCP-anti-CD8 and PE-anti-CD4 mAbs. The sorted cell populations were of more than 99% purity through FACS reanalysis. Platelets were isolated from citrate-treated blood by centrifugation at 160 g for 10 min to give platelet-rich plasma and by further centrifugation at 1100 g for 10 min to obtain a platelet pellet.

Chemotaxis assay

A chemotaxis assay was performed as described elsewhere [25]. Chemotactic activity is expressed as migration index (MI), i.e. the number of cells migrated to mPBP divided by the number of the cells migrated to the negative control (with medium in the lower well only). In all cases, each chemotaxis assay was performed in triplicate wells and each MI value was the average of the three experimental results, with the mean value shown and the error bars representing the sample standard deviation. For pertussis toxin (PTX; Sigma) blockage, thymocytes (2×10^6/ml) were pretreated with 1.0 μg/ml PTX in complete medium for 90 min at 37 °C. After incubation, the cells were washed and resuspended in fresh medium for the assessment of chemotaxis.

Stable expression of recombinant mouse CXCR2 in HEK293 cells

To amplify the complete encoding region of murine CXCR2 cDNA, primers were designed: forward, 5′-CCGGATCCTCAAAGATGGGAGAATTCAAGGTG-3′ (136–159); reverse, 5′-GGTCTAGAGGTGAACAGTCTTTAGAGGGTAGTAGAG-3′ (1233–1206). The *Bam*HI and *Xba*I restriction sites were introduced into the forward and the reverse primer, respectively (underlined). The PCR condition was: 94 °C, 2 min; 94 °C, 30 s, 60 °C, 30 s, 72 °C, 2 min, for 30 cycles; followed by 72 °C extension for 3 min. The PCR product was directionally cloned into the pcDNA3 eukaryotic expression vector (Invitrogen, Carlsbad, Calif.). The constructed plasmids were sequenced to confirm the absence of PCR-introduced point mutation. HEK293 cells were grown in six-well plates to 80% confluence, then transfected with 5 μg pcDNA3-CXCR2 reconstructed plasmids using transfectin reagent (Promega). Mock transfection with 5 μg pcDNA3 plasmid into HEK293 cells was performed as control. The stable transfectants resistant to 1 mg/ml G418 (Life Technologies, Carlsbad, Calif.) were screened and the individual colonies picked up by limiting dilution. The expression of murine CXCR2 in the transfected cell clones was confirmed by Northern blot, as well as by staining the cells with anti-mouse CXCR2 pAb and analyzed on FACS.

Northern blot analysis

The expression of mPBP in fMTSCs was determined by Northern blot (NB). Two micrograms mRNA isolated from fMTSCs was fractionated by electrophoresis on 1% agarose-formaldehyde gels, blotted onto nylon filters (Hybond-N^+, Amersham Biotech, Uppsala, Sweden), and cross-linked by baking at 80 °C for 2 h. The membranes were prehybridized for 4 h at 65 °C in 6 × sodium chloride/sodium citrate buffer (SSC), 2 × Denhardt's solution, 0.5% sodium dodecylsulfate (SDS), 100 μg/ml sheared salmon sperm DNA. Hybridization was performed in the same conditions for 18 h on addition of mPBP cDNA probe labeled with [α-^{32}P]dCTP. After stringent washing, the filters were exposed to X-ray films for autoradiography. The detection of CXCR2 expression in gene-transfected HEK293 cells was performed similarly, except that the mRNA was extracted from CXCR2– and mock-transfected HEK293 cells, and the probe was labeled from the fragment of the coding region of CXCR2.

Calcium flux analysis

$CXCR2^+$ HEK293 cells, mock-transfected HEK293 cells and PMNs (5×10^6/ml) were washed twice with balanced saline solution (BSS)-2% FCS and then incubated in 10% FCS-DMEM in the dark with the calcium indicator FLUO-3/AM (Biotium, Hayward, Canada) at a final concentration of 1.0 μM, with addition of 0.01% pluronic F-127 (Biotium) at 37 °C for 60 min [26]. After incubation, recombinant mPBP protein (100 ng/ml) was added and calcium mobilization was measured by flow cytometry. The excitation wavelength was 488 nm and the emission was measured at 526 nm. In parallel experiments, mouse CXCL2/3/MIP-2 (50 ng/ml) protein was used as a positive control. A PTX blockage assay was performed by pretreating cells with PTX (1.0 μg/ml) at 37 °C for 90 min prior to the addition of mPBP or CXCL2/3/MIP-2.

In situ hybridization

Sense and antisense digoxigenin (DIG)-labeled cRNA probes of mPBP were synthesized using a DIG RNA la-

beling kit (Roche Diagnostics). The template was the *Eco*RI/*Xba*I-digested fragment containing the open reading frame (ORF) cDNA of mPBP constructed in the pcDI vector. The antisense probe was generated by SP6 transcription of an *Eco*RI-linearized template, and the sense probe by T7 transcription of an *Xba*I-linearized template. The frozen sections of mouse thymus were fixed in 4% paraformaldehyde for 20 min at room temperature (RT). The sorted thymic Mo/Mϕs or Mo/Mϕ-depleted thymic stromal cells were adhered to slides by Cytospan centrifugation, then fixed. DIG-labeled cRNA (0.5 μg/ml) of either sense or antisense probe was added into the hybridization mixture (50% formamide, 10% dextran sulfate, 20 mM Tris-HCl, pH 8.0, 1 mM EDTA, 300 mM NaCl, 1 × Denhardt's solution, 250 μg/ml yeast tRNA, 100 mM DTT and 100 μg/ml salmon sperm DNA). After overnight incubation at 50 °C, the sections or slides were washed with 2 × SSC, 50% formamide for 30 min at 37 °C, and treated with 10 μg/ml RNase A. After washing of the residual RNase A, the sections were incubated with AP-conjugated anti-DIG Ab (1:1000). Color development was performed with nitroblue tetrozulium (NBT; 400 μg/ml), 5-bromo-4-chloro-3-indolyl phosphate (BCIP; 200 μg/ml) at RT in the dark. The slides were rinsed in 10 mM Tris-HCl (pH 8.0) plus 1 mM EDTA to stop the color reaction. The slides were covered with a coverslip and sealed with 50% glycerol gelatin for microscopic visualization. The negative control was the hybridization of template with sense RNA probe.

Coimmunoprecipitation and Western blot analysis

CXCR2-transfected HEK293 cells (5×10^6) and mock-transfected HEK293 cells were stimulated with recombinant mPBP (200 ng/ml) at 37 °C for 1 min. The cells were rinsed with PBS, scraped and pelleted. Cell lysates were prepared with lysis buffer (20 mM Tris, pH 8.0, 150 mM NaCl, 1 mM EDTA, 1% Triton, 10 μg/ml leupeptin, 10 μg/ml aprotinin and 1 mM phenylmethylsulfonyl fluoride) for 30 min at 4 °C, then centrifuged (12,000 g, 10 min) to collect the supernatant. Immunoprecipitations were performed with rabbit anti-mPBP pAb (5 μg/ml), followed by protein A-Sepharose. After washing three times with the lysis buffer containing 500 mM NaCl, the immunoprecipitates from CXCR2-transfected HEK293 cells or mock-transfected HEK293 cells were separated on 12.5% SDS-PAGE and transferred to nitrocellulose membranes. Western blot analysis was performed with goat anti-CXCR2 pAb. After incubation with AP-conjugated anti-goat IgG, the color development was performed with NBT/BCIP.

Reverse transcription-polymerase chain reaction

mPBP expression in thymic Mo/Mϕs was determined by RT-PCR. One microgram total RNA extracted from sorted thymic Mo/Mϕs, Mo/Mϕ-depleted thymic stromal cells, peritoneal Mo/Mϕs, fMTSCs, total thymus cells or platelets was treated with RNase-free DNase I (Promega), reverse transcribed into first-strand cDNAs with RT-for-PCR kit (BD Biosciences Clontech, Pato Alto, Calif.). For the detection of mPBP expression, the primers used were: forward, 5′-GCTCAGCCTCACGTTGTTCCC-3′ (positions 25–45); reverse, 5′-CAGATGAAGCAG CTGGTCAGTAACC-3′ (positions 443–419). PCR was performed on a 9700 Thermal Cycler PCR machine (Perkin Elmer, Foster City, Calif.) in a standard 50-μl Taq polymerase reaction mixture (Promega) containing 50 ng of first-strand cDNA, 0.2 mM of each of the dNTPs,10 pmol of forward or reverse primer, and 3U Taq polymerase. The PCR condition was: 94 °C, 2 min; 94 °C, 30 s; 55 °C, 30 s; 72 °C, 1 min, for 30 cycles; 72 °C extension for 2 min. β-actin was used as an internal control to normalize the possible differences in the amount of cDNA synthesized. The primers to amplify β-actin were: forward, 5′-TGGAATCCTGTGGCATCCATGAAAC-3′; reverse, 5′-TAAAA-CGCAGCTCAGTAACAGTCCG-3′. The detection of Mac-1 mRNA was applied to verify the presence or absence of thymic Mo/Mϕs in distinct cell populations. The primer pairs used to amplify mouse Mac-1 mRNA were: 5′-CTCTGTGGACATGGACGCTG-3′ and 5′-TGCTGAGATCGTCTTGGCAG-3′.

Immunohistochemistry

Immunohistochemistry (IHC) was applied to identify CXCR2-expressed cells in thymus. The frozen mouse thymuses were cut into consecutive sections with a thickness of 4 μm, fixed in 4% paraformaldehyde for 10 min, then rinsed twice with PBS. The thymus sections were first incubated with normal rabbit serum diluted 1:50 for 30 min at RT to block the non-specific binding sites, then incubated with 1:500 diluted goat anti-CXCR2 pAb, or goat serum as negative control, for 30 min at RT. Having been rinsed in PBS, the sections were incubated with HRP-conjugated anti-goat IgG (1:1000) for 30 min at RT. Following three washes with PBS, the sections were subjected to color development using the substrate 3, 3′-diaminobenzidine (DAB) according to the manufacturer's instruction. Sections were counterstained with Mayer's hematoxylin and mounted with glycerol-gelatin for microscopic visualization. To determine the cell types of mPBP mRNA+ cells in thymus identified by in situ hybridization (ISH), thymus frozen sections of odd number were used for ISH and the sections of even number used for IHC. For IHC, the primary Abs were rat anti-mouse DEC205, anti-mouse Mac-1 and cell culture supernatants of ER-TR4, 5, and 7 mAbs. To demonstrate the production of mPBP by thymic Mo/Mϕs, the sorted thymic Mo/Mϕs were cytospun onto glass slides and stained with rabbit anti-mPBP pAbs, followed by HRP-conjugated anti-rabbit IgG and color development with the addition of DAB as the substrate.

Real-time PCR to quantitate CXCR2 mRNA expression in thymocyte subsets

To quantitate the CXCR2 expression in the four subsets of thymocytes, real-time fluorescence PCR was performed in an iCycler instrument (Bio-Rad, Hercules, Calif.) through monitoring the increase in fluorescence by the binding of SYBR Green (PE Applied Biosystems Division, Foster City, Calif.) to double-stranded DNA. Plasmids containing CXCR2 cDNA or the β-actin cDNA fragment in a series of tenfold dilutions were used as templates to draw a standard curve. The cDNA templates were prepared from mouse tissues or from FACS-sorted thymocytes subsets. The primers used for the cDNAs were mouse CXCR2: forward, 5′-TCACAAACAGCGTCGTAGAAC-3′; reverse, 5′-TATGCACACAAACTTGACAAG-3′, which spans an intron of CXCR2 (*Mus musculus* chromosome 1, 52104635-52108855); β-actin: forward, 5′-TGGAATCCT GTGGCATCCATGAAAC-3′; reverse, 5′-TAAAACGCA GCTCAGTAACAGTCCG-3′. Melt-curve analysis was performed to determine the temperature where data were collected. All PCR reactions were carried out in triplicate with positive and negative controls using the standard program. Correlation coefficients of standard curves above 0.99 assure the accuracy of the data. The PCR cycling conditions were as follows: 94 °C for 2 min, and 40 cycles of 94 °C for 20 s, 60 °C for 5 s and 72 °C for 40 s, with a single fluorescence measurement immediately after the extension of each cycle at 84 °C for 8 s. Quantification of CXCR2 mRNA expression was determined by calculating the expression index (EI) to represent the relative expression abundance of CXCR2 standardized by β-actin, i.e. the mRNA EI = (copy numbers of CXCR2 mRNA/copy numbers of β-actin mRNA) × 1000 AU (arbitrary units). The PCR products were resolved in a 1.5% agarose/EB gel to confirm the specificity.

Results

mPBP cDNA encodes an ELR$^+$ CXC chemokine

In fMTSCs, mPBP was expressed as two distinct transcripts of 1.1 and 0.7 kb, of which the former was dominant as shown in NB (fig. 1A). Both cDNAs contain an identical open reading frame of 342 nucleotides and encode a protein of 113 amino acids (aa). mPBP protein contains a signal peptide of 40 aa (fig. 2, underlined). The predicted mature protein consists of 73 aa with 8 aa immediately upstream of the ELR motif. The conserved four cysteines are located in the appropriate positions with an arginine between the first two cysteines (fig. 2). At the amino acid level, the predicted mPBP protein has 50.4% and 73% identity to human and rat PBP, respectively.

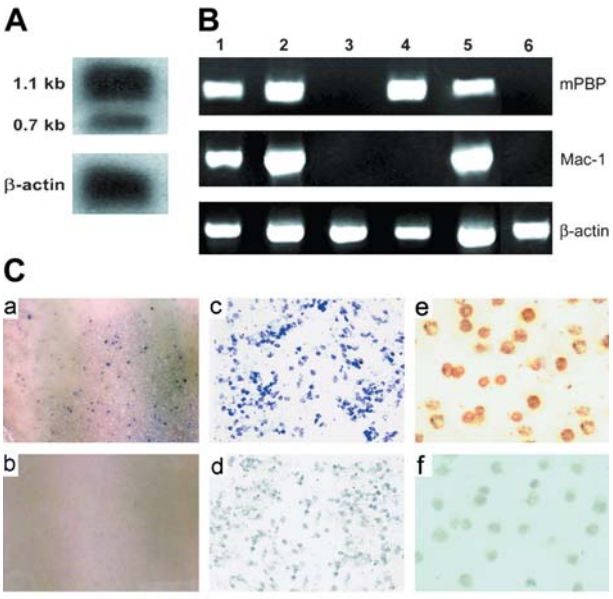

Figure 1. Localization of mPBP in thymus and expression in thymic Mo/Mϕs. (*A*) NB analysis of the expression of mPBP mRNA in fMTSCs. Two transcripts of 1.1 and 0.7 kb were displayed. β-actin was used as an internal control. (*B*) Detection of mPBP mRNA expression in thymic Mo/Mϕs by RT-PCR. Lane 1, fMTSCS; 2, thymic Mo/Mϕs; 3, Mo/Mϕ-depleted thymic stromal cells; 4, platelets; 5, peritoneal Mo/Mϕs; 6, thymocytes. Isolated thymic Mo/Mϕs and Mo/Mϕ-depleted stromal cells were prepared as described in Materials and methods. β-actin was used as an internal control to normalize the possible differences in the amount of cDNA synthesized. Mac-1 was amplified as a molecular marker to verify the presence or absence of Mo/Mϕs in different cell populations. (*C*) Mouse PBP expression in thymus and purified thymic Mo/Mϕs. In ISH, the expression of mPBP mRNA was visualized as scattered in the cells located mainly in the thymic medulla, and in the thymic cortex as well as in the corticomedullary junction (a, indigo color, original magnification ×100). Purified thymic Mo/Mϕs showed a positive signal in the hybridization with the antisense mPBP probe (c, original magnification ×200), but negative using a sense probe (b, thymic section; d, purified thymic Mo/Mϕs). The production of mPBP by thymic Mo/Mϕs was demonstrated by IHC. FACS-sorted thymic Mo/Mϕs were adhered to glass slides by cytospinning and stained with anti-mPBP pAb, followed by staining with HRP-labeled goat anti-rabbit Ab: color was then developed with DAB. The mPBP protein was shown in thymic Mo/Mϕs (e, original magnification ×400). Preimmune rabbit serum was used as negative control (f, original magnification ×400).

Expression of mPBP mRNA and protein in thymic Mo/Mϕs

The expression of mPBP in thymus was detected in fMTSCs and thymic Mo/Mϕs (fig. 1B, lanes 1, 2), but not in Mo/Mϕ-depleted thymic stromal cells (fig. 1B, lane 3), suggesting that mPBP may be produced by thymic Mo/Mϕs. To further investigate the nature of mPBP-producing cells and their localization in thymus, ISH was performed. In thymus frozen sections, mPBP mRNA was localized mainly in the corticomedullary junction and thymic medulla, with a small portion in the thymic cortex. The positive cells showed a scattered dis-

Figure 2. Alignment of the amino acid sequences between mPBP, hPBP and rat PBP (AAK30166). Conserved amino acids are shadowed. The NH_2 terminal truncated products of hPBP, CTAP-III, β-TG and NAP-2 are marked with vertical lines to show the cleavage sites. The ELR motif and the four conserved cysteines are indicated with panels. The signal peptide of mPBP is underlined. MO, mouse; HU, human; RA, rat.

tribution (fig. 1C, a). Thymus sections in IHC staining adjacent to those used in ISH with anti-mouse ER-TR4, 5 and 7, DEC-205 and Mac-1 mAbs indicated that only Mac-1^+ cells matched topographically to the mPBP mRNA$^+$ cells in ISH (data not shown). This indicated that the mPBP-producing cells are probably thymic Mo/Mϕs. To confirm this, thymic Mo/Mϕs were isolated from thymus and subjected to ISH and IHC assays. The results indicated that the isolated thymic Mo/Mϕs exhibited clear positive signals in the hybridization with mPBP antisense cRNA probe (fig. 1C, c), as well as in the staining with anti-mPBP pAb (fig. 1C, e). Hybridization to sense cRNA probes and staining to irrelevant antiserum gave no signals (fig. 1C, d, f).

Chemotactic activity of recombinant mPBP protein to immune cells

The reconstructed pQE-30-mPBP plasmids were transformed into M15 host bacteria and the expression of mPBP mature protein was induced by IPTG (1 mM). mPBP was expressed in both inclusion bodies and cytosol in *Escherichia coli* with a MW of 9 kDa (fig. 3A). The soluble mPBP with 6 × His fused at the NH_2 terminus in cytosol was purified by a Ni-NTA affinity column. Mouse PBP protein was chemotactic to various types of immune cells with different potencies (fig. 3B). The chemotactic effect of mPBP was robust for PMNs (MI = 11.7 ± 1.2, in 1.0 μg/ml), potent for peritoneal monocytes (MI = 7.3 ± 0.5, in 2.0 μg/ml) and less potent to spleen lymphocytes (MI = 4.5 ± 0.4, in 1.0 μg/ml). The chemotactic activity of mPBP to the target cells was in a dose-dependent fashion. mPBP was less potent at 2.0 μg/ml than at 1.0 μg/ml in chemotaxis for PMNs or splenic lymphocytes (fig. 3B). A similar phenomenon has been observed for MDC and SDF-1 [27, 28]. Such phenomena may be attributed to the internalization of ligand-receptor complex and subsequent receptor desensitization. Additionally, migration in response to mPBP was abolished by pretreatment of each cell type with 1.0 μg/ml PTX (data not shown), suggesting that mPBP-induced chemotaxis is via the coupling of the receptor to a Gαi protein to initiate a signaling pathway.

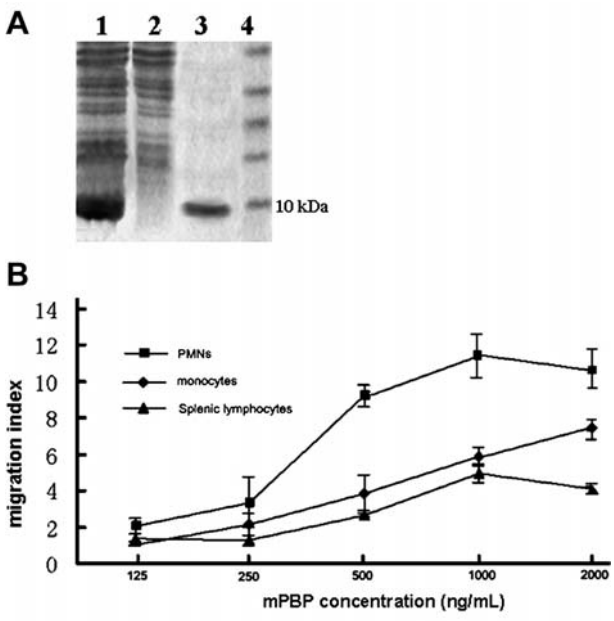

Figure 3. Chemotaxis of recombinant mPBP protein for immune cells. (*A*) Expression and purification of recombinant mPBP. Recombinant mPBP protein with the 6 × His tag at the NH_2 terminus was expressed in *E. coli* after IPTG induction and purified with a Ni-NTA affinity column. Lane 1, bacteria lysate after induction; lane 2, bacteria lysate before induction; lane 3, purified mPBP protein; lane 4, protein molecular-weight standards. (*B*) The mPBP protein was chemoattractive for PMNs, peritoneal monocytes and splenic lymphocytes in a dose-dependent manner. All experiments were repeated three times and the mean ± SD is shown.

CXCR2 is a cognate receptor for mPBP

The receptor specific for mPBP has not been identified. In the human system, two receptors CXCR1 and CXCR2 cognate to ELR$^+$ CXC chemokines have been discussed. The receptor for hPBP and its derivatives connective tissue-activating peptide III (CTAP-III), beta-thromboglobulin (β-TG) and NAP-2 is CXCR2 [19]. In mouse, only the functional homologue of CXCR2, but not that of CXCR1, has been identified so far [29] and binding of CXCL1/KC and CXCL2/3/MIP-2 to CXCR2$^+$ PMNs is important for PMN migratation to the inflammatory site [15, 30, 31]. As the receptor for hPBP and its derivative NAP-2, CXCR2 is predicted to be the receptor for mPBP, and this was confirmed in our study. We established CXCR2-expressing stable clones in HEK293 cells, which do not normally express CXCR2 (fig. 4A). The expression of recombinant CXCR2 protein in transfected HEK293 cells was confirmed by flow cytometry (fig. 4B). The biological signaling generated immediately after the ligand binding to the cognate receptor was monitored in the calcium flux assay. Mouse CXCL2/3/MIP-2 was used as a positive control for chemokine-induced biologic activity [19]. In our assay, CXCL2/3/MIP-2 (50 ng/ml) induced a calcium flux in PMNs and CXCR2+ HEK293 cells (fig. 4C). In the mPBP-induced calcium

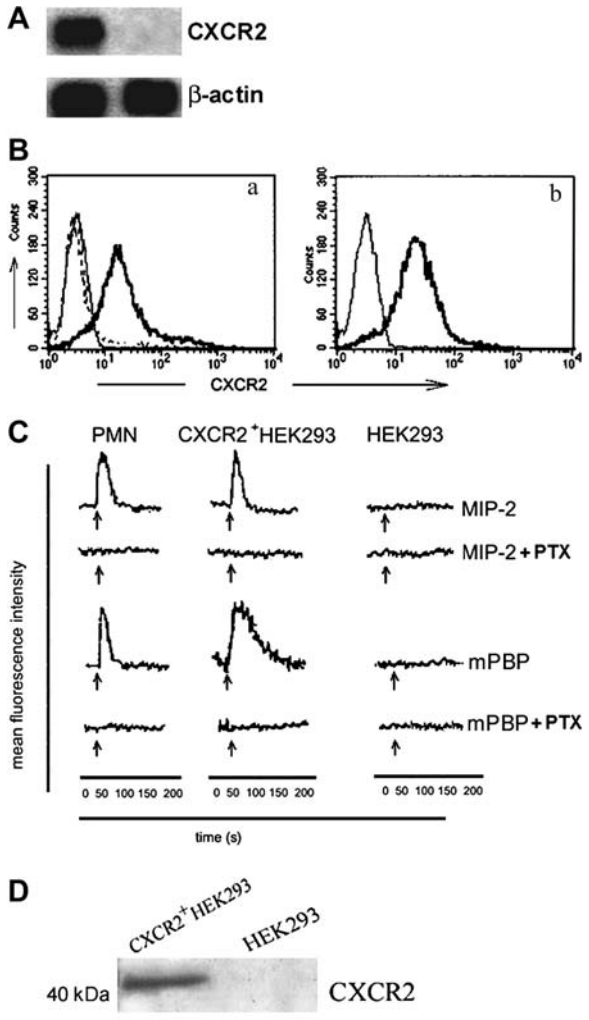

Figure 4. CXCR2 is a cognate receptor for mPBP. (*A*) NB analysis shows CXCR2 mRNA expression in gene-transfected HEK293 cells (left) but not in mock-transfected HEK293 cells (right). β-actin was used as an internal control. (*B*) FACS analysis of CXCR2 protein in gene-transfected HEK293 cells. The CXCR2-gene-transfected and mock-transfected HEK293 cells, as well as the isolated PMNs were stained with goat anti-mouse CXCR2 pAb, then analyzed by flow cytometry. In panel a, the CXCR2 protein was expressed on CXCR2-gene-transfected HEK293 cells (solid line), but not on mock-transfected HEK293 cells (thin line); the cells stained with isotype control IgG were negative (dotted line). In panel b, the PMNs were CXCR2 positive (solid line). The control isotype control IgG staining is shown as a thin line. (*C*) mPBP induced a calcium flux in $CXCR2^+$ HEK293 cells. The cells pretreated with FLUO-3/AM were stimulated with mPBP (100 ng/ml) and CXCL2/3/MIP-2 (50 ng/ml). The mean fluorescence intensity was measured to show the calcium mobilization in CXCR2-gene-transfected 293 cells and PMNs, as well as in mock-transfected 293 cells. A PTX blockage assay was performed by pretreating the cells with PTX (1.0 μg/ml) at 37 °C for 90 min before the addition of chemokines and the measurement of calcium influx. (*D*) Interaction of mPBP with CXCR2 in gene-transfected HEK293 cells. Both $CXCR2^+$ HEK293 cells and mock-transfected HEK293 cells were stimulated with mPBP (200 ng/ml). Cell lysates were immunoprecipitated with anti-mPBP pAb. The immunoprecipitates were analyzed by Western blot with anti-CXCR2 pAb. A clear blot band with the proper MW for CXCR2 was shown in the product immunoprecipitated from the lysate of $CXCR2^+$ HEK293 cells, whereas there was no such band in the lysate of mock-transfected HEK293 cells.

flux assays, addition of mPBP (100 ng/ml) to the FLUO-3/AM-pretreated PMNs and $CXCR2^+$ HEK293 cells induced a sharp increase in the calcium flux (fig. 4C). In the negative control, addition of CXCL2/3/MIP-2 or mPBP to FLUO-3/AM-pretreated mock-transfected HEK293 cells, the calcium concentration was maintained at a basal level during the entire recorded period (fig. 4C). Furthermore, the mPBP/CXCR2-induced calcium flux was blocked by pretreatment with PTX (1.0 μg/ml, fig. 4C). Evidently, CXCR2 is a cognate receptor for mPBP. To further determine whether mPBP interacts with CXCR2 directly, we stimulated CXCR2-transfected HEK293 cells and mock-transfected HEK293 cells with an appropriate dose of recombinant mPBP (200 ng/ml). We then performed coimmunoprecipitation with anti-mPBP antibody and Western blot analysis with anti-CXCR2 antibody. A clear blot band with the proper MW of CXCR2 was shown in the product immunoprecipitated from the lysate of $CXCR2^+$ HEK293 cells, whereas there was no such band in the lysate of mock-transfected HEK293 cells (fig. 4D). The results indicated that mPBP could directly bind to CXCR2.

CXCR2 expression on the surface of four major subsets of thymocytes

In IHC assays with frozen sections, CXCR2-positive cells were distributed in both thymic cortex and medulla (fig. 5A). In FACS analysis, the expression of CXCR2 on four definded subsets by CD4 and CD8 was 38.8%, 28.0%, 12.8% and 17.6% in DN, DP, CD4SP and CD8SP thymocytes, respectively (fig. 5B). The intensity of expressed CXCR2 was highest in DN, moderate in DP and CD8SP and low in CD4SP thymocytes.

To quantitate CXCR2 mRNA expression in the four subsets of thymocytes, real-time fluorescence PCR was performed. The expression abundance of CXCR2 was calculated and expressed as an EI value. As shown in table 1, the abundance of CXCR2 mRNA expression in four major thymocyte subsets was in the order DN>DP>CD8SP>CD4SP thymocytes, which correlated with the

Table 1. Quantitative analysis of CXCR2 expression on thymocyte subsets and PMNs.

Cell sub-populations	Copy number		
	CXCR2 ($\times 10^2$)	β-actin ($\times 10^3$)	EI*
DN	12.34	8.60	143
DP	4.67	6.34	74
CD4SP	4.27	10.11	42
CD8SP	5.80	9.94	58
Thymocytes	5.92	8.24	73
PMNs	18.23	8.07	226

* EI = (copy numbers of CXCR2 mRNA/copy numbers of β-actin mRNA) × 1000 AU (arbitrary units).

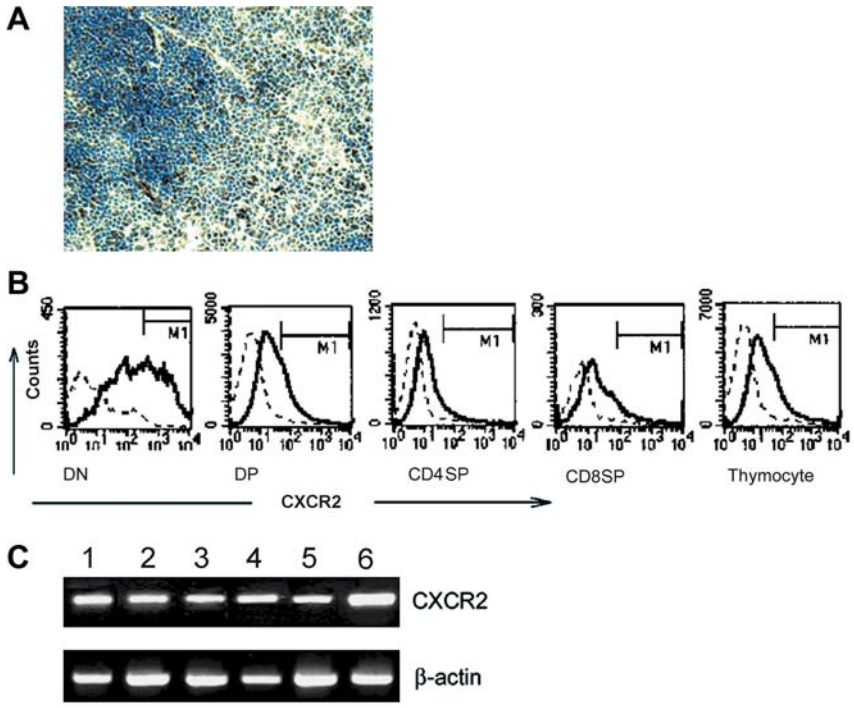

Figure 5. CXCR2 expression on the surfaces of thymocytes of major subsets. (*A*) IHC staining of mouse thymus frozen sections showed that CXCR2 was diffusely expressed in thymic cortex and medulla (brown color, original magnification ×200). (*B*) Three-color analysis of thymocytes stained with rabbit anti-goat CXCR2 pAb, followed by anti-rabbit IgG-FITC, anti-CD4-PE and anti-CD8-PerCP. The intensity of CXCR2 on each subset of thymocytes is shown as a solid line in comparison with the corresponding subset stained with the IgG isotype controls (dotted line). (*C*) Products of real-time RT-PCR to detect CXCR2 mRNA expression were verified on an agarose/EB gel. Mouse thymocytes were labeled with anti-CD4-PE and anti-CD8-PerCP, then sorted on FACS into DN, DP $CD4^+$SP and $CD8^+$SP subsets with a purity of 99%. RNA was extracted from each subset and reverse transcribed into cDNA. The primers used to amplify the CXCR2 spanned an intron of CXCR2 chromosome sequence to exclude the contamination of genomic DNA. Lane 1, DN; lane 2, DP; lane 3, CD4SP; lane 4 CD8SP; lane 5, total thymocytes; lane 6, PMNs. β-actin was used as internal control.

protein expression levels in the respective thymocyte subsets, but was substantially lower than that in PMNs. The PCR products were verified by electrophoresis to show the specificity of amplification (fig. 5C). The ratios of CXCR2 versus β-actin seemed not so distinct as those calculated from the values of threshold cycle (CT) in the real-time PCR assay. This may due to the saturation of the amplification reaction after 40 cylces.

Chemotactic effects of mPBP on thymocyte subsets

To examine the chemotactic effects of mPBP on thymocyte subsets, DN, DP, CD4SP and CD8SP thymocytes were isolated and purified by FACS sorting (fig. 6A) and used immediately as target cells for the migration attracted by chemokines in 48-well microchambers. All four major thymocyte subsets migrated in response to mPBP protein in a dose-dependent manner (fig. 6B). The minimal concentration of mPBP to induce chemotaxis for DN and DP thymocytes was 250 ng/ml ($p < 0.05$). At the mPBP concentration of 1000 ng/ml, the migration index was 3.7, 4.3, 2.2 and 3.8 for DN, DP, CD4SP and CD8SP thymocytes, respectively. However, the optimal dose of mPBP for the maximal migration varied among different subsets: the optimal dose for DN thymocytes was 2000 ng/ml, with an MI of 5.3; for DP and CD8SP thymocytes it was 1000 ng/ml, with an MI of 4.3 and 3.8, respectively; for CD4SP thymocytes it was 500 ng /ml, with an MI of 2.8. The potency of chemotactic activity of mPBP for the four thymocyte subsets was in the order of DN>DP>CD8SP>CD4SP, correlating with the respective levels and intensities of CXCR2 expressed by the respective thymocyte subsets. This migration did not occur when mPBP protein was added in both upper and lower components of the microchambers, excluding the possibility of chemokinetic activity. Chemotaxis of thymocytes to mPBP was completely abolished by pretreatment of thymocytes with PTX (fig. 6B), confirming that the signal was generated through binding of mPBP to CXCR2 and activating PTX-sensitive Gαi protein to induce chemotaxis for thymocytes.

The thymocytes were sorted into $CXCR2^+$ and $CXCR2^-$ groups by FACS and their responses to mPBP (1.0 μg/ml) were compared with that to CXCL2/3/MIP-2 (200 ng/ml) as positive control. The recombinant mPBP showed significantly higher chemotaxis for the $CXCR2^+$ thymocytes than for total thymocytes, while virtually no chemo-

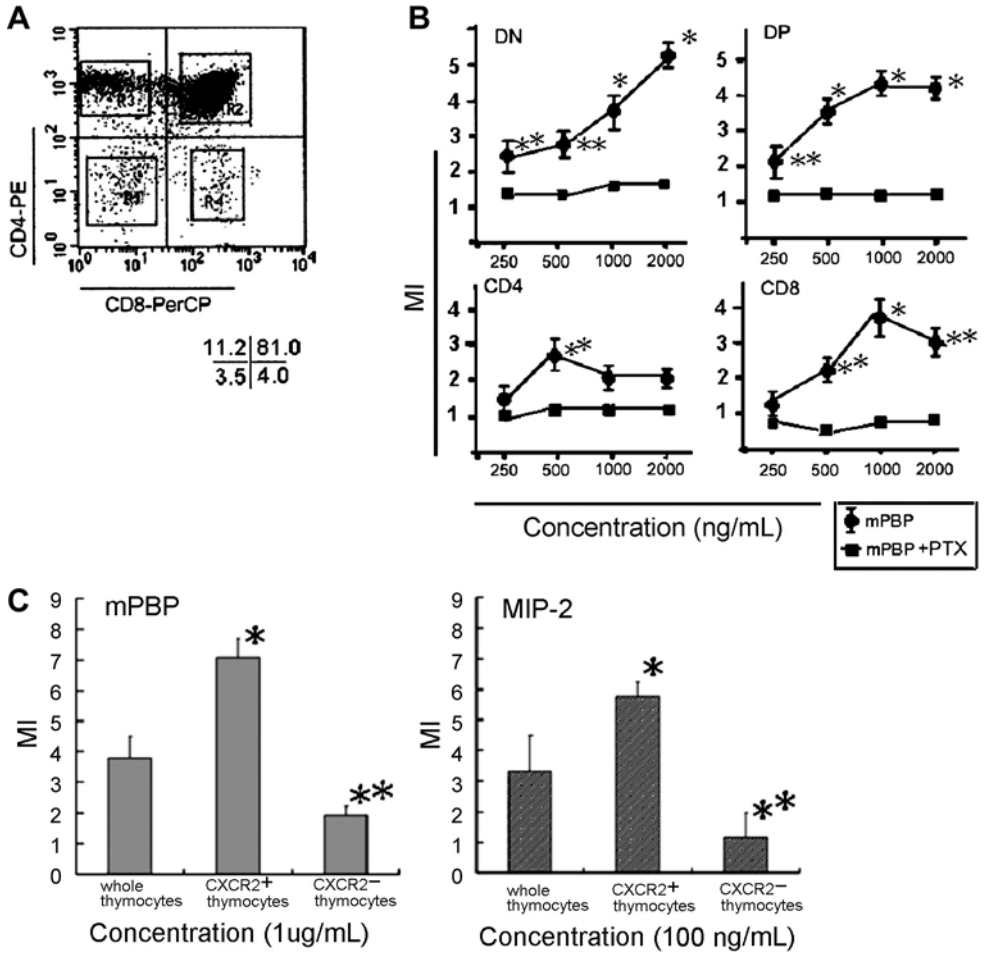

Figure 6. Migration capacity of thymocytes of purified subsets in response to mPBP. (*A*) Four- to 6-week-old mouse thymocytes, stained with anti-CD4-PE and anti-CD8-PerCP, were sorted into DN, DP, CD4SP and CD8SP subsets by flow cytometry. The gates for the sorting of each thymocyte subset are shown and the purity of the thymocytes in each sorted subset was 99%. (*B*) Chemotaxis of mPBP for the sorted thymocyte subsets. Each test point represents the mean ± SD of the MI, the number of the cells migrated to mPBP divided by the number of the cells migrated to medium only. The chemotaxis of each time point was performed in triplicate. All experiments were repeated at least twice. The chemotactic activity was significantly higher in response to mPBP in the cells without PTX pretreatment than for the cells with PTX pretreatment (*$p < 0.01$, **$p < 0.05$). (*C*) The mouse thymocytes were sorted by FACS into $CXCR2^+$ and $CXCR2^-$ groups and their responses to mPBP (1.0 µg/ml) and MIP-2 (200 ng/ml) by migration were analyzed. In comparison with the chemotaxis for total thymocytes, the mPBP showed higher chemotaxis for the $CXCR2^+$ thymocytes (*$p < 0.01$); while virtually no chemotaxis for the $CXCR2^-$ thymocytes (**$p < 0.01$) was seen. Similar patterns of chemotaxis for thymocytes were also shown in response to CXCL2/3/MIP-2.

taxis for the $CXCR2^-$ thymocytes was observed (fig. 6C). The results were comparable to those for chemoattraction by CXCL2/3/MIP-2. This supports CXCR2 as a cognate receptor of mPBP, with thymocyte migration mediated through this pairing of chemokine receptor and ligand.

Discussion

The ELR^+ CXC chemokine mPBP is produced by thymic Mo/Mϕs. A previous report showed that mPBP was specifically expressed by bone-marrow-derived megakaryocytes and spleen [23]. In this study, we cloned mPBP from thymic stromal cells. The cultured fMTSCs, from which the mPBP cDNA was cloned, consisted of cortical and medullary types of thymic epithelial cells, thymic Mo/Mϕs and fibroblasts. However, thymic dendritic cells died and degraded after a 3-week in vitro cultivation, while other types of blood cells were washed off during the preparation of the fMTSCs. To identify the type(s) of thymic stromal cells which produce mPBP, ISH was applied in conjunction with IHC on thymic frozen sections. The mPBP $mRNA^+$ cells were dispersed, mainly in the thymic medulla areas, and to some extent in the corticomedullary junction and cortex (fig. 1C, a). In the separate staining with various mAbs specific against cortical type-, medullary type-thymic epithelial cells, thymic dendritic cells, thymic Mo/Mϕs and fibroblasts, the ISH^+ cells were topologically matched only with the Mac-1^+ cells (Mo/Mϕs). This was confirmed by RT-PCR

using RNA extracted from purified thymic Mo/Mϕs (fig. 1B). Accordingly, the thymic Mo/Mϕs are the cells expressing mPBP within mouse thymus. Moreover, the mouse peritoneal Mo/Mϕs expressed mPBP mRNA (fig. 1B). These data suggest that mPBP is not megakaryocyte/platelet-specific, and can be produced by other types of cells, such as Mo/Mϕs in thymus and the periphery. The failure to detect mPBP mRNA in thymus by NB at the organ level [23] may be attributed to the too low proportion of thymic Mo/Mϕs, approximately 0.01% of total thymus cells.

Mature hPBP and mPBP have distinct chemotactic activities. Mature hPBP exhibits little chemotactic activity for PMNs. It needs a posttranslational modification to generate NH_2-terminal truncated forms of CTAP III or β-TG, both of which mount substantial chemotaxis for PMNs. These intermediate products are further cleaved to generate NAP-2, which is a potent chemokine for PMNs [32]. In contrast, the recombinant mPBP mature protein lacking the NH_2-terminal signal peptide exhibited robust chemoattractant activity for PMNs. The difference may be explained by the fact that the length of the NH_2-terminal amino acid sequence adjacent to the ELR motif is different among the various truncated forms of hPBP. Mature hPBP is longer than hNAP-2 by 24 aa; in contrast, mature mPBP is 4 and 8 aa shorter than respective hβ-TG and hCTAP III, while being only 7 aa longer than hNAP-2 (fig. 2). Hence, the NH_2-terminal amino acids adjacent to the ELR motif possibly have inhibitory effects on the chemotactic activity of PBP.

In this report, we identified CXCR2 as a cognate receptor for mPBP on the following evidence. (i) mPBP was chemoattractant for and induced calcium influx in CXCR2-transfected HEK293 cells and these activities could be entirely blocked by pretreating the cells with PTX (fig. 4C). (2) mPBP could bind to CXCR2 as revealed by coimmunoprecipitation and Western blot (fig. 4D). In our assays, mPBP was a chemokine robust for PMNs, potent for Mo/Mϕs and less potent for spleen lymphocytes (fig. 3B). The fact that mPBP was less chemotactic for splenic lymphocytes may correlate with the low proportion (21.3%) of mouse spleen $CXCR2^+$ T cells in our flow cytometry analysis, the figure being comparable to, but slightly higher than the 11% of $CXCR2^+$ T cells in human peripheral blood [33].

Since mPBP is expressed in thymic Mo/Mϕs, we subsequently analyzed CXCR2 expression on the four major subsets of thymocytes of the adult BALB/c mice. Our results suggest that CXCR2 is detectable in all four major subsets of thymocytes, with a higher level in DN thymocytes. These results are inconsistent with a previous report [34]. In that report, CXCR2 protein was undetectable on thymocytes and $CD4^+$, $CD8^+$ and $B220^+$ lymphocytes in peripheral blood and spleen. These conflicting results may be due to the use of different antibodies in the respective experiments. A polyclonal antibody against full-length CXCR2 was used in the previous study [34]. In our assay, we used a polyclonal antibody raised against the NH_2 terminal 17 aa in the extracellular domain of mouse CXCR2 [35, 36]. This antibody has been shown to recognize membrane-associated native CXCR2 protein [35, 36].

Our finding that mPBP, similar to CXCL12/SDF-1, is a potent chemokine for DN thymocytes implies that these two chemokines may have functional redundancy to ensure the directional migration of thymocyte progenitors and the early stages of DN thymocytes. Furthermore, mPBP exhibited more broad chemotactic activity than the CXCL12/SDF-1, as it attracts the four major thymocyte subsets though with different potencies, suggesting that mPBP is an important chemokine functioning in thymus. In addition, the thymic Mo/Mϕs are generally regarded as the cells involved in thymic negative selection, acting as scavengers to clean the apoptotic cells. Our demonstration that thymic Mo/Mϕs can produce mPBP may extend the biologic activity of these cells within thymus.

Acknowledgements. This work was supported by grants from ICGEB CRP/CHN98-02, China National 973 Program No. G1999053904 and China NSFC grant (30330520). Many thanks to Drs R. M. Strieter (UCLA) and W. van Ewijk (Erasmus University) for kindly giving us Abs. We also thank Prof. B. Zhang and L. Hou for the technical supports in ISH and J. P. Tao and S. L. Ma for FACS sorting. W. X. Fu and S. Y. Gong contributed equally to this work.

1 Baggiolini M., Dewald B. and Moser B. (1997) Human chemokines. Annu. Rev. Immunol. **15:** 675–705
2 Lindley I. J. D., Westwick J. and Kunkel S. L. (1993) Nomenclature announcement: the chemokines. Immunol. Today **14:** 24
3 Jason G. C. (1999) Chemokines and cell migration in secondary lymphoid organs. Science **286:** 2098–2102
4 Broxmeyer H. E., Sherry B., Lu L. and Cooper S. (1989) Myelopoietic enhancing effects of murine macrophage inflammatory protein 1 and 2 on colony formation in vitro by murine and human bone marrow granulocyte/macrophage progenitor cell. J. Exp. Med. **170:** 1583–1594
5 Cocchi F., DeVico A. L., Garzino-Demo A., Arya S. K., Gallo R. C. and Lusso P. (1995) Identification of RANTES, MIP-1a, and MIP-1b as the major HIV-suppressive factors produced by $CD8^+$ T cells. Science **270:** 1811–1815
6 Wilson S., Mendes-da-Cruz D. A., Silva J. S., Dardenne M. and Cotta-de-Almeida V. (2002) Intrathymic T-cell migration: a combinatorial interplay of extracellular matrix and chemokines? Trends Immunol. **23:** 305–313
7 Shirozu M., Nakano T. and Inazawa J. (1995) Structure and chromosomal localization of the human stromal cell-derived factor 1 (SDF-1) gene. Genomics **28:** 495–500
8 Zaitseva M. B., Lee S. and Rabin R. L. (1998) CXCR4 and CCR5 on human thymocytes: biological function and role in HIV-1 infection. J. Immunol. **161:** 3103–3113
9 Suzuki G., Sawa H. and Kobayashi Y. (1999) Pertussis toxin-sensitive signal controls the trafficking of thymocytes across the corticomedullary junction in the thymus. J. Immunol. **162:** 5981–5985
10 Annunziato F., Romagnani P. and Cosmi L. (2000) Macrophage-derived chemokine and EBI1-ligand chemokine

attract human thymocytes in different stages of development and are produced by distinct subsets of medullary epithelial cells: possible implications for negative selection. J. Immunol. **165:** 238–246
11 Taylor J. R. Jr, Kimbrell K. C., Scoggins R., Delaney M., Wu L. and Camerini D. (2001) Expression and function of chemokine receptors on human thymocytes: implications for infection by human immunodeficiency virus type 1. J. Virol. **75:** 8752–8760
12 Xie L. P., Qian X. P., Gong S. Y. and Chen W. F. (2000) Analysis on the types of chemokines expressed by the murine thymic epithelial cell line MTEC1. Chin. Sci. Bull. **45:** 1098–1101
13 Chantry D., Romagnani, P., Raport C. J., Wood C. L., Epp A., Romagnani S. et al. (1999) Macrophage-derived chemokine is localized to thymic medullary epithelial cells and is a chemoattractant for CD3(+), CD4(+), CD8(low) thymocytes. Blood **94:** 1890–1898
14 Campbell J. J., Pan J. and Butcher E. C. (1999) Cutting edge: development switches in chemokine responses during T cell maturation. J. Immunol. **163:** 2353–2357
15 Cacalano G., Lee J., Kikly K., Ryan A. M., Meek S. P., Hultagren B. et al. (1994) Neutrophil and B cell expansion in mice that lack the murine IL-8 receptor homolog. Science **265:** 682–684
16 Nagasawa T., Hirota S., Tachibana K., Takaku N., Nishikawa A., Kitamura Y. et al. (1996) Defects of B-cell lymphopoiesis and bone-marrow myelopoiesis in mice lacking the CXC chemokine PBSF/SDF-1. Nature **382:** 635–638
17 Zou Y. R., Kottmann A. H., Kuroda M., Taniuchi I. and Littman D. R. (1998) Function of the chemokine receptor CXCR4 in haematopoiesis and in cerebellar development. Nature **393:** 595–599
18 Forster R., Schubel A., Breitfeld D., Dremmer E., Renner-Muller I., Wolf E. et al. (1999) CCR7 coordinates the primary immune response by establishing functional microenvironments in secondary lymphoid organs. Cell **99:** 23–33
19 Wuyts A., Proost P., Lenaerts J.-P., Ben-Baruch A., Van Damme J. and Wang, J. M. (1998) Differential usage of the CXC chemokine receptors 1 and 2 by interleukin-8, granulocyte chemotactic protein-2 and epithelial-cell-derived neutrophil attractant-78. Eur. J. Biochem. **255:** 67–73
20 Kim C. H. and Broxmeyer H. E. (1999) SLC/Exodus/6Ckine/TCA4 induces chemotaxis of hematopoietic progenitor cells: differential activity of ligands of CCR7, CXCR3, or CXCR4 in chemotaxis vs. suppression of progenitor proliferation. J. Leukoc. Biol. **66:** 455–461
21 Romagnani P., Annunziato F. and Lazzeri E. (2001) IP-10, Mig and I-TAC are produced by thymic epithelial cells and attract TCR$\alpha\beta$+CD8+ single-positive T cells, TCR$\gamma\delta$+ T cells and NK-type cells in human thymus. Blood **97:** 601–607
22 Zhang C. Y., Thornton A. A., Kowalska A. A., Sachies B. S., Feledman M., Mortimer M. et al. (2001) Localization of distal regulatory domains in the megakaryocyte-specific platelet basic protein/platelet factor 4 gene locus. Blood **98:** 610–617
23 Oda M., Haruta H., Nagao M. and Nagata Y. (2002) Isolation and characterization of mouse homolog of the neutrophils activating peptide-2. Biochem. Biophys. Res. Commun. **290:** 865–868
24 Ge Q. and Chen W. F. (2000) Effect of murine thymic epithelial cell line (MTCK1) on the functional expression of CD4+CD8+ thymocyte subgroups. Int. Immunol. **12:** 1127–1133
25 Fu W. X., Zhu M. L., Gong S. Y., Li Y. and Chen W. F. (2004) Molecular cloning and characterization of a novel rat CXC chemokine, rPBP, the homologue of human and mouse PBP. Cytokine **26:** 37–43
26 Kao J. P. Y., Harootunian A. T. and Tsien R. Y. (1989) Photochemically generated cytosolic calcium pulses and their detection by Fluo-3. J. Biol. Chem. **264:** 8179–8184
27 Godiska R., Chantry D., Raport C. J., Sozzani S., Allavena P., Leviten D. et al. (1997) Human macrophage-derived chemokine (MDC), a novel chemoattractant for monocytes, monocyte-derived dendritic cells, and natural killer cells. J. Exp. Med. **185:** 1595–1604
28 Poznansky M. C., Olszak I. T., Foxall R., Evans R. H., Luster A. D. and Scadden D. T. (2000) Active movement of T cells away from a chemokine. Nat. Med. **6:** 543–548
29 Cerretti D. P., Nelson N., Kozlosky C. J., Morrissey P. J., Copeland N. G., Gilbert D. J. et al. (1993) The murine homologue of the human interleukin-8 receptor type B maps near the Ity-Lsh-Bcg disease resistance locus. Genomics **18:** 410–413
30 Lee J., Cacalano G., Camerato T., Toy K., Moore M. W. and Wood W. I. (1995) Chemokine binding and activities mediated by the mouse IL-8 receptor. J. Immunol.**155:** 2158–2164
31 Bozic C. R., Gerard N. P., Uexkull-Guldenband C., Kolakowski L. F., Conklyn M. J. Jr, Breslow R. et al. (1994) The murine interleukin 8 type B receptor homologue and its ligands: expression and biological characterization. J. Biol. Chem. **269:** 29355–29358
32 Wuyts A., D'Haese A., Cremers V., Menten P., Lenaerts J.-P., Loof A. D. et al. (1999) NH-2- and COOH-terminal truncations of murine granulocyte chemotactic protein-2 augment the in vitro and in vivo neutrophils chemotactic potency. J. Immunol. **163:** 6155–6163
33 Inngjerdingen M., Damaj B. and Maghazachi A. A. (2001) Expression and regulation of chemokine receptors in human natural killer cells. Blood **97:** 365–375
34 Wang J. B., Zhang Y., Kasahara T., Harada A., Matsushima K. and Mukaida N. (1996) Detection of mouse IL-8 receptor homologue repression on peripheral blood leukocytes and mature myeloid linage cells in bone marrow. J. Leukoc. Biol. **60:** 372–381
35 Ness T. L., Hogaboam C. M., Strieter R. M. and Kunkel S. L. (2003) Immunomodulatory role of CXCR2 during experimental septic peritonitis. J. Immunol. **171:** 3775–3784
36 Mehrad B., Strieter R. M., Moore T. A., Tsai W. C., Lira S. A. and Standiford T. J. (1999) CXC chemokine receptor-2 ligands are necessary components of neutrophil-mediated host defense in invasive pulmonary aspergillosis. J. Immunol. **163:** 6086– 6094